BNL-26547

Projectile Rapidity Dependence in Target Fragmentation*

P. E. Haustein, J. B. Cumming, and H.-C. Hseuh

Chemistry Department, Brookhaven National Laboratory, Upton, NY 11973

Abstract

The thick-target, thick-catcher technique has been used to determine mean kinetic properties of selected products of the fragmentation of Cu by ^{1}H, ^{4}He, and ^{12}C ions (180-28000 MeV/amu). Momentum transfer, as inferred from F/B ratios, is observed to occur most efficiently for the lower velocity projectiles. Recoil properties of target fragments vary strongly with product mass, but show only a weak dependence on projectile type. The projectile's rapidity is shown to be a useful variable for quantitative intercomparison of different reactions. These results indicate that E_{proj}/A_{proj} is the dominant parameter which governs the mean recoil behavior of target fragments.

*Work performed at Brookhaven National Laboratory under the auspices of the U.S. Department of Energy and supported by its Office of Basic Energy Sciences.

DISCLAIMER

One of the fundamental motivations for studying the interactions of heavy ions at intermediate energies is to delineate the features of the nuclear reaction mechanism(s). A systematic examination of heavy-ion reactions in the 10 to 200 MeV/amu energy range will connect our extensive knowledge of the low energy region (E < 10 MeV/amu) which is characterized by transfer, compound nuclear, and deeply inelastic scattering processes and our somewhat more limited studies of the fully relativistic energy region, (E > GeV/amu). Here there are some indications that asymptotic behavior has been observed in peripheral reactions and where there is currently strong interest in central collisions for the possibility that these may prove useful for inducing nuclear shock waves, producing states of abnormally high nuclear density, or as a means of defining the nuclear equation of state under conditions away from those (presently accessible) of near-equilibrium. It is convenient to systematize[1] the nuclear reaction mechanism in the manner shown in Fig. 1 by using the variables of projectile energy and reaction impact parameter. One does not expect abrupt changes to occur in crossing the cross hatched boundaries of Fig. 1 but rather it is reasonable to assume that heavy-ion interactions in the intermediate energy region will reflect transitions from one or more of these domains to different ones. One expects that the nuclear physics in this energy range will be at least as interesting and varied as that at both low and high energy extremes and that it will challenge us to design experiments which are sensitive to the new phenomena and to have as goals the development of theoretical models to interpret them.

Research efforts of nuclear chemists at BNL have been directed toward these points for the last several years. It is a reflection of the successful acceleration of heavy ions to fully relativistic energies that we are approaching the intermediate energy region from the higher energy side

rather than from the lower energy side! From the broad new areas of investigations which have developed from the use of these high energy heavy ion beams,[2] I will restrict my remarks to a consideration of target fragmentation processes.

In a historical sense our studies of target fragmentation by high-energy heavy ions grew out of the long tradiation in the BNL Chemistry Department of similar investigations with GeV protons. In particular, many of the experimental techniques and methods of interpretation which will be emphasized later in this talk had their origins in early experiments at proton synchrotrons where one frequently had to contend with high energy proton beams of very low intensity. In the quarter century since protons were first accelerated to GeV energies in the now-retired Cosmotron, a large number of target systems have been investigated at various laboratories at energies up to 400 GeV. These studies have involved radiochemical techniques, detection in mica and Lexan, and electronic measurements of fragments by dE/dX, E, and time of flight. There is, therefore, a sizable body of information in the literature on the interaction of GeV protons with complex nuclei. Building upon this base one can therefore inquire as to whether relativistic heavy ions differ from protons in their interactions with complex nuclei.

In the areas of target fragmentation, as opposed to projectile fragmentation where there is no analog in proton induced reactions, our studies have developed from a "first generation" series of experiments which concentrated on the systematics of production cross sections to a series of "second generation" studies of mean recoil properties of the target fragments. In the former case we were interested in testing the applicability to relativistic heavy-ion reactions of the hypothesis of limiting fragmentation and factorization[3] and in the latter case we have attempted to extend these

tests in the area of fragment recoil behavior and to explore to what extent the kinetic properties of target fragments are complementary to those observed previously in projectile fragmentation. Our studies also bear upon a central question in studies of the nuclear reaction mechanism: whether the projectile's kinetic energy or its velocity (related to E/A) is the dominant parameter which characterizes the major features of the interaction.

As a means of orientation to the discussion which follows, it is useful to locate our studies of target fragmentation on the heavy-ion reaction "phase diagram" (Fig. 1). Our measurements concern target fragments which result from medium to large impact parameter. Table I lists the beams we have used at various laboratories in the investigations of reactions with Cu targets. Our measurements refer to the upper, right-hand portion of the phase diagram.

A variety of studies with targets ranging from Cu to U and using residual radioactivity techniques have shown that various relativistic heavy ions (^{4}He, ^{12}C, ^{20}Ne, ^{40}Ar), 0.4-2 GeV/amu, produce essentially the same distribution of final products as do protons of GeV energies.[4-10] The relativistic heavy-ion reactions exhibit larger reaction cross sections than those for protons, but the distribution of products (except for very light ones) scales in proportion to this larger geometrical cross section. These observations, while somewhat surprising at such relatively low energies, support the hypotheses[3] of limiting fragmentation and factorization, which in their simplest application to nuclear reactions suggest that, at sufficiently high energy, all strongly interacting projectiles will yield similar product distributions. As an example of this, Fig. 2 shows ratios of product cross sections for the reactions of 80 GeV ^{40}Ar and 28 GeV ^{1}H

with Cu.[7] The cross-hatched band shows the region consistent with the ratio of total reaction cross sections and its associated error. The factoring of the individual product cross sections according to the ratio of the total reaction cross sections for 28 GeV ^{1}H and 80 GeV ^{40}Ar on Cu is a general feature for products which correspond to the removal of up to $\simeq$40 nucleons from the target (i.e. down to ^{22}Na). Still lighter products, e.g. ^{7}Be, appear to be significantly enhanced for the heavy-ion induced reaction over the proton induced one. Data of the type shown in Fig. 2 can be used to develop both charge dispersion and mass yield plots as shown in Figs. 3 and 4, respectively. The charge dispersion analysis shows that the data for ^{40}Ar + Cu fall on the same curve as those for ^{1}H + Cu and that the mass yield curves for 80 GeV ^{40}Ar, 25 GeV ^{12}C, and 28 GeV ^{1}H reactions on Cu have essentially the same shape and slope for all three projectiles. The slope of the mass yield curve is related to excitation energy which is delivered to the target nucleus. Low excitation energy (rapidly decreasing cross section for increasing multinucleon removal, ΔA) is correlated with large slope of the mass yield curve, while high excitation energy (less rapid decrease in cross section as ΔA increases) is correlated with smaller slope. Figure 5 shows this variation in slope for Cu spallation by protons and energetic heavy ions. At $\simeq$1-2 GeV we see the onset of a saturation phenomenon in that the Cu target is no longer able to absorb additional excitation energy, and at even higher energies the fragmentation pattern is not changed by either different projectile types or their kinetic energy. Similar data are not yet available for heavier target systems. It would be interesting to know, for example, if heavier target systems show the same limiting slope behavior at $\simeq$1-2 GeV, or whether this occurs at higher

energy due to the ability of heavier targets to support more excitation as a result of their greater mass.

While limiting fragmentation behavior has also been observed[3] in the Cu target systems with lower energy ^{14}N (280 MeV/amu), it is clear that the strict factorization of the cross sections as shown in Fig. 2 will eventually break down at some lower projectile energy when deeply inelastic scattering, compound nucleus formation, or other processes become the dominant reaction mechanisms. It is therefore of considerable fundamental interest to explore the energy region below $\approx$200-300 MeV/amu to see where the cross section factorization regime fails and to inquire whether this failure is observed at approximately the same projectile energy or velocity for all projectile-target combinations.

Models of the interaction of relativistic heavy ions (such as the abrasion-ablation model[11]) suggest a monotonic relationship (on the average) between impact parament and reaction product, with the simplest (smallest mass loss) being associated with the largest b, and vice versa. Based on the procedure of Barshay et al.[12,13] in which

$$d\sigma_R = 2\pi b\{1 - \exp[-T(b)\sigma_{NN}^T]\}db,$$

we have calculated the contributions of different ranges of impact parametets to σ_R. In this equation, T(b) is the thickness function [as defined by Eq. (2,3) of Ref. 13] which includes all the geometrical properties of the colliding nuclei, and σ_{NN}^T is the spin and isospin-averaged nucleon-nucleon cross section at 2 GeV/nucleon. This calculation predicts that impact parameters of $\approx$8.2 fm make the largest contributions to σ_R. For closer approaches, the nuclei are black to each other and the b term in the above equation is dominant. For larger b, transparencies become significant,

rapidly reducing the contributions, yet some reactions at impact parameters in the 10-12-fm range are expected. We note that the most effective impact parameters are larger than the sum of the half-density radii of ^{40}Ar and $^{63,65}Cu$, 3.39 and 4.23 fm, respectively, so that peripheral collisions are expected to play important roles. Impact parameters $\gtrsim$8.3 fm contribute a cross section equal to the estimated yields of products with A $\geq$ 58, the upturning region of the mass yield curve in Fig. 4. Furthermore, the $\approx$2160 mb deduced for target fragmentation residues having A $\geq$ 22 are accounted for by collisions with b $\geq$ 5.25 fm. Shown in Fig. 6 are realistic nuclear density distributions for Cu and ^{40}Ar at this impact parameter. There is little overlap of the central cores of the projectile and target even at this separation and in this sense target fragmentation is peripheral. Major parts of the Ar and Cu remain relatively undisturbed to ultimately yield the fragmentation products. Presumably events with smaller b and greater overlap will result in increasingly violent interactions.

A more detailed view of heavy-ion reaction mechanisms in the intermediate-energy region can be obtained from the measurement of the energy and momentum transfer processes of these interactions. It is in these areas that our work has concentrated most recently. Because of the limitations imposed by low beam intensities, the thick target, thick catcher technique which was originally developed for high energy proton beams has been employed to survey the momentum transfer to target fragments from Cu for a variety of proton and heavy-ion projectiles over a broad energy range. Figures 7 and 8 show typical configurations of target stacks that are used in these experiments. Fragments which recoil from the Cu target are stopped in Mylar catchers. The quantities F and B denote the fractions of the activity of a particular nuclide formed in a Cu target of w mg/cm^2 thickness that were found

in the forward and backward catchers, respectively, of the stack perpendicular to the beam.

Before we try to interpret the results of such measurements in a detailed way which requires a model for the interaction, it is instructive to look merely at the ratio of F/B for several products from Cu. We have chosen to use ^{24}Na, ^{28}Mg, ^{44m}Sc, ^{48}V, ^{52}Mn, and ^{58}Co as a convenient set of products, distributed in mass, which have both abundant γ-rays in their decays for identification purposes and long enough half-lives so their yields can be determined readily by assay of residual radioactivity following the target stack bombardment. These products, in a crude way, also sample a range of excitation energies in the heavy-ion interaction in that a product like ^{58}Co which is formed by the removal of a few nucleons from Cu represents only modest excitation of the target while ^{24}Na formed by the loss of ≈ 40 nucleons from Cu results from the deposition of larger amounts of excitation energy into the target.

The ratios of F/B for several different projectile-energy combinsations are listed in Table II. We also include earlier data from Crespo et al.[14] As expected, the ratios are greater than unity, indicating that more of the products are found in the forward hemisphere, ahead of the target, than behind it. For a particular product, a smooth trend of decreasing F/B ratio is evident if the table is ordered by E_{proj}/A_{proj} (related to the square of the projectile velocity) rather than by the total kinetic energy of the projectile. Since the F/B ratio reflects the extent of momentum transfer from projectile to target, it is apparent that the projectile's velocity and not its type (proton, alpha, or ^{12}C) is the governing factor in the momentum transfer process. For a particular projectile-energy combination the F/B ratio generally increases with increasing product mass and then drops appreciably

for ^{58}Co. The drop for the ^{58}Co data is presumed to be a reflection of changes in the range-energy relationship for low-velocity near-target products like ^{58}Co. It is clearly of interest to extend these measurements to lower projectile velocities to explore more fully the processes which are responsible for the momentum transfers we see here. It would also be instructive to include both additional types of projectiles as well as other targets to get a more complete picture of these phenomena.

Additional information can be obtained from the present data by a model dependent analysis which assumes that the velocity distribution of a product can be resolved into two components (see Fig. 8), a forward directed $v_{||}$ resulting from the initial projectile-target interaction, and a V isotropic in the moving system, arising from the subsequent deexcitation of the prefragment to yield the observed products. This so-called two-step model is equivalent to the abrasion-ablation model[11] proposed for high-energy, heavy-ion reactions. Details of how $v_{||}$ and V are derived from the experimental data can be found in the review article of Alexander[15] and elsewhere.[16] The mean range R is related to 2w(F+B), and w(F-B) is related to $\eta_{||}R$, where $\eta_{||} = v_{||}/V$. It is also assumed that the mean range is related to V through an exponential dependence, $R \propto V^N$.

Figures 9 and 10 show plots of $\beta_{||} = v_{||}/c$ and V, respectively, that were derived from our data. It is convenient and informative to plot these results as a function of the rapidity y ($=\tanh^{-1}\beta$) of the projectile. A number of interesting features are apparent from these figures. For a given projectile-energy combination $\beta_{||}$ varies strongly with product mass, higher values of $\beta_{||}$ being observed for the lighter products (e.g. ^{24}Na), and smaller values of $\beta_{||}$ for the near-target products (e.g. ^{58}Co). The observed values of $\beta_{||}$ are low and of the same order as the velocity retardation reported for

projectile fragments.[17] We are therefore observing complementary behavior in the projectile and target fragmentation regimes which reflects the indistinguishability of the two interacting nuclei in their center of mass frame. This suggests that fragments even as light as ^{24}Na arise from relatively unexcited parts of the target nucleus. One also notes that $\beta_{||}$ varies monotonically with respect to the number of nucleons removed from the target. For a given product $\beta_{||}$ increases rapidly for the slower moving projectiles, which indicates that the lower velocity projectiles transfer their momenta more effectively to the target system. The plots of V (Fig. 10) give us some insight into the degree of excitation in the prefragments which are assumed to deexcite by light particle evaporation to yield the final products, shown in the figure. For a given projectile-energy combination we again see that the lighter products display the higher velocity behavior we saw in the $\beta_{||}$ results and that variation of V with product mass is remarkably similar to Fig. 9. However, the variation of V with projectile rapidity (velocity) is quite small with just a hint of the beginnings of an upturn for 720 MeV ^{4}He (180 MeV/amu). The $\beta_{||}$ results suggest that heavy-ion projectiles at low rapidity (E/A $\approx$ 200-400 MeV/amu) are effective in transferring momentum to excited prefragments by projecting them forward in the initial projectile-target interaction. The excitation of the prefragments, however, as inferred from V, does not seem to correlate well with either the type of energy of the incident projectile. Fully relativistic heavy ions, e.g. 25 GeV ^{12}C, reveal only small differences when compared to high energy (28 GeV) protons, in accord with concepts of limiting, asymptotic behavior mentioned earlier.

The results from reactions with Cu target system cannot, in themselves, form a basis for constructing a detailed model of the interaction of heavy nuclei at intermediate to high energies. Clearly one needs to investigate

reactions with other targets in a similar way. Investigations with Au targets have been reported[18] recently and other investigations with Ag,[19] Ta, and U[20] targets are in progress. Clearly, the measurements of product angular distributions and energy spectra will give us the comprehensive, detailed information which is crucial for testing, refining, or rejecting theoretical models of the mechanisms of these heavy-ion interactions. Unfortunately the low intensity of the presently available beams makes experiments of this type very difficult.

In summary, the use of heavy ions of intermediate energy holds the promise of providing a means for the systematic study of target fragmentation processes with the eventual goal of refining models of the mechanism(s) of the interaction of heavy nuclei in this bridging energy region. In particular a number of fundamental questions can be addressed:

(1) At what projectile energy (or velocity) will the predictions of limiting fragmentation and factorization break down? What will be responsible for this breakdown? Will it occur at the same projectile energy (or velocity) for all projectile-target systems?

(2) Why are the recoil properties of target fragments, such as momentum transfer, closely correlated with projectile rapidity (velocity) instead of the projectile's total energy? Will this occur in other projectile-target systems? Will this correlation continue at lower velocities?

(3) Will projectile-target systems of large mass asymmetry (e.g. very light projectiles like π-mesons or heavy-ion projectiles of mass greater than the target) display the same features of the systems already studied?

(4) Is the two-step (abrasion-ablation) model valid over a wide energy range? Will it break down at lower energies? What will be the cause of this and what will be the signature of the new processes which take over at these energies?

(5) What are the best measurements to perform in the next generation of experiments so that additional constraints can be applied to refining theoretical models of the interaction of heavy nuclei at intermediate energies?

[1]J. P. Bondorf, Workshop on High Resolution Heavy-Ion Physics at 20-100 MeV/nucleon, Saclay, France, 1978.

[2]A. S. Goldhaber and H. H. Heckman, Ann. Rev. Nucl. Sci. 28, 161 (1978).

[3]See the review by H. Bøggild and T. Ferbel, Ann. Rev. Nucl. Sci. 24, 451 (1974).

[4]J. B. Cumming, P. E. Haustein, R. W. Stoenner, L. Mausner, and R. A. Naumann, Phys. Rev. C 1-, 739 (1974).

[5]C. R. Rudy and N. T. Porile, Phys. Lett. 59B, 240 (1975).

[6]J. B. Cumming, R. W. Stoenner, and P. E. Haustein, Phys. Rev. C 14, 1554 (1976).

[7]W. Loveland, R. J. Otto, D. J. Morrissey, and G. T. Seaborg, Phys. Lett. 69B, 284 (1977).

[8]J. B. Cumming, P. E. Haustein, T. J. Ruth, and G. J. Virtes, Phys. Rev. C 17, 1632 (1978).

[9]W. Loveland, R. J. Otto, D. J. Morrissey, and G. T. Seaborg, Phys. Rev. Lett. 39, 320 (1977).

[10]N. T. Porile, G. D. Cole, and C. R. Rudy, Phys. Rev. C 19, 2288 (1979).

[11]J. D. Bowman, W. J. Swiatecki, and C. F. Tsang, Lawrence Berkeley Report No. LBL-2908, 1973 (unpublished).

[12]S. Barshay, C. B. Dover, and J. P. Vary, Phys. Lett. 51B, 5 (1974).

[13]S. Barshay, C. B. Dover, and J. P. Vary, Phys. Rev. C 11, 360 (1975).

[14]V. P. Crespo, J. M. Alexander, and E. K. Hyde, Phys. Rev. 131, 1765 (1963).

[15]See the review by J. M. Alexander, in Nuclear Chemistry, edited by L. Yaffe (Academic, New York, 1968), Vol. I, p. 273.

[16]J. B. Cumming, P. E. Haustein, and H.-C. Hseuh, Phys. Rev. C 18, 1372 (1978).

[17]D. E. Greiner, P. J. Lindstrom, H. H. Heckman, B. Cork, and F. S. Bieser, Phys. Rev. Lett. 35, 152 (1975).

[18]S. B. Kaufman, E. P. Steinberg, and B. D. Wilkins, Phys. Rev. Lett. 41, 1359 (1978).

[19]N. T. Porile (private communication).

[20]W. Loveland (private communication).

Table I

Proton and Heavy-Ion Beams used in the Study of the Spallation of Cu Targets

Ion	E (MeV)	E/A (MeV/amu)	Laboratory
^{4}He	720	180	SREL
^{14}N	3900	280	PPA
^{12}C	4800	400	LBL
^{4}He	4000	1000	LBL
^{40}Ar	80000	2000	LBL
^{12}C	25200	2100	LBL
^{1}H	3900	3900	BNL
^{1}H	28000	28000	BNL

Table II

F/B Ratios of Selected Target Fragments from the Spallation of Copper by Various Projectiles

Projectile	Energy (MeV)	Energy / A (MeV/A)	F/B ^{24}Na	^{28}Mg	^{44}Sc	^{48}V	^{52}Mn	^{58}Co
^{4}He	720	180	9.1 (25)	--	29.6 (20)	23.1 (33)	35.5 (35)	14.7 (35)
^{4}He[a]	880	220	8.23(29)	8.80(66)	--	--	--	--
^{12}C	4800	400	8.62(22)	8.41(72)	12.8 (03)	12.3 (04)	11.4 (03)	6.42(03)
^{1}H[a]	700	700	3.37	4.13	--	--	--	--
^{4}He	4000	1000	4.25(29)	2.83(68)	4.86(19)	4.31(59)	4.05(30)	2.96(50)
^{12}C	25200	2100	2.63(11)	2.69(34)	3.37(12)	3.21(19)	3.21(26)	2.62(29)
^{1}H[a]	3000	3000	2.79	3.02	--	--	--	--
^{1}H	28000	28000	2.20(05)	2.20(11)	2.77(06)	2.72(06)	2.82(06)	2.36(10)

[a]Reference 14.

Figure Captions

1. A "Phase Diagram" for the Heavy Ion Reactions (from Reference 1). Reactions which are induced by heavy ions with energies of 10-200 MeV/A are expected to exhibit some or all of the features in the central part of the diagram.

2. Cross section ratios vs product mass for the reactions of 80-GeV ^{40}Ar and 28-GeV ^{1}H with Cu. The cross hatched band shows the region consistent with the ratio of total reaction cross sections and its associated error.

3. Comparison of charge dispersion curves for the spallation of Cu by 80-GeV ^{40}Ar and 28-GeV ^{1}H. Points were obtained by the procedure described in Reference 6.

4. Mass yield curves for the spallation of Cu by 80-GeV ^{40}Ar, 25-GeV ^{12}C (Reference 6), and 28-GeV ^{1}H (Reference 6). The vertical scale for ^{12}C is arbitrary. Points were obtained using the procedure of Reference 6 by adding computer generated values for non-observed products to the measured cross sections. These are filled when >50% of the total was observed, open when >20% observed. Errors include 20% uncertainties assumed in the calculated values.

5. Slope of the Cu spallation mass-yield curve as a function of the kinetic energy of the incident projectile. Filled circles are for protons, open for heavy ions as indicated.

6. Nuclear density distributions for Cu and ^{40}Ar showing the extent of overlap when the separation of centers if 5.25 fm.

7. Pictorial view of a typical thick-target/thick-catcher irradiation geometry. The beam enters from the left and first transverses a target at 90° to the beam. The beam then passes through a similar target stack which is inclined at 20° to the beam direction.

8. Schematic view of the thick-target/thick catcher assembly. The lower portion of the figure shows the resolution of the velocity vector of a target fragment into an initial $v_{||}$ resulting from the projectile-target interaction and a V (assumed to be isotropic) resulting from the deexcitation of excited prefragments which eventually yield the observed products.

9. Dependence of $\beta_{||}$ (= $v_{||}/c$), the first (abrasion) step velocity, as a function of projectile rapidity for several target fragments from Cu.

10. Dependence of V the second (ablation) step velocity, as a function of projectile rapidity for several target fragments from Cu.

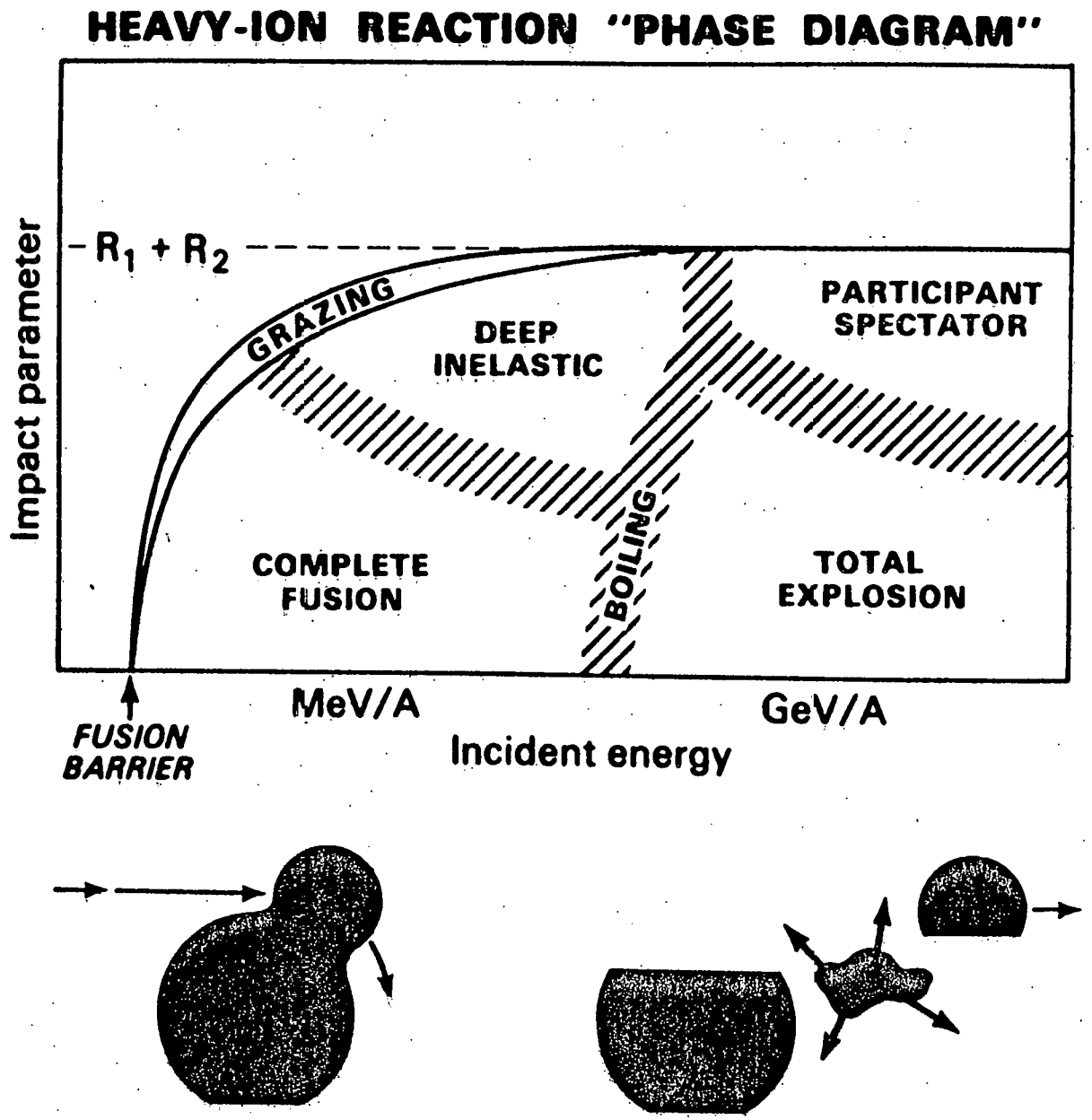
HEAVY-ION REACTION "PHASE DIAGRAM"
Impact parameter
$R_1 + R_2$
GRAZING
DEEP INELASTIC
PARTICIPANT SPECTATOR
COMPLETE FUSION
BOILING
TOTAL EXPLOSION
FUSION BARRIER
MeV/A
GeV/A
Incident energy

Fig. 1

7-72-79

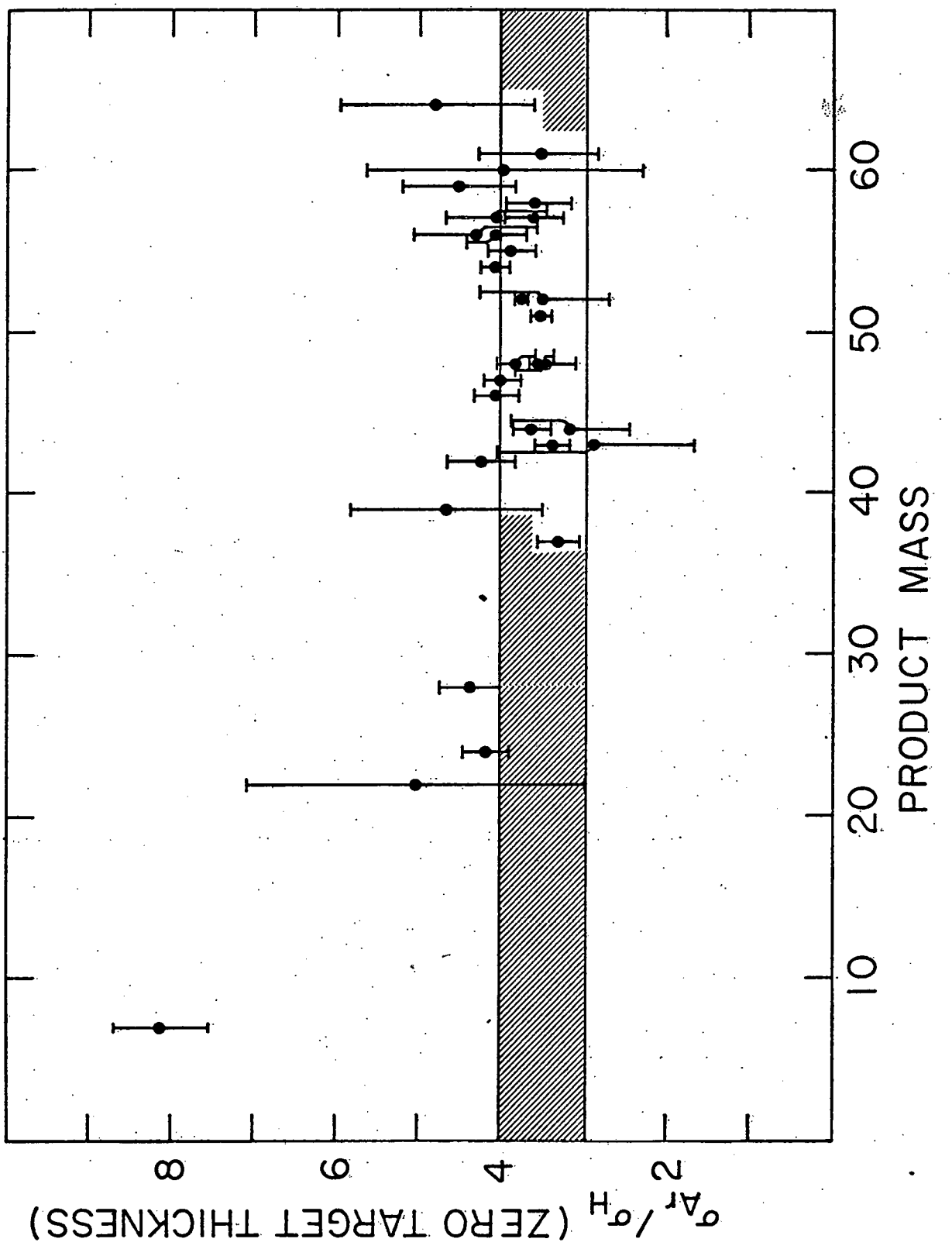
PRODUCT MASS
10
20
30
40
50
60
σ_{Ar}/σ_H (ZERO TARGET THICKNESS)
2
4
6
8

Fig. 2

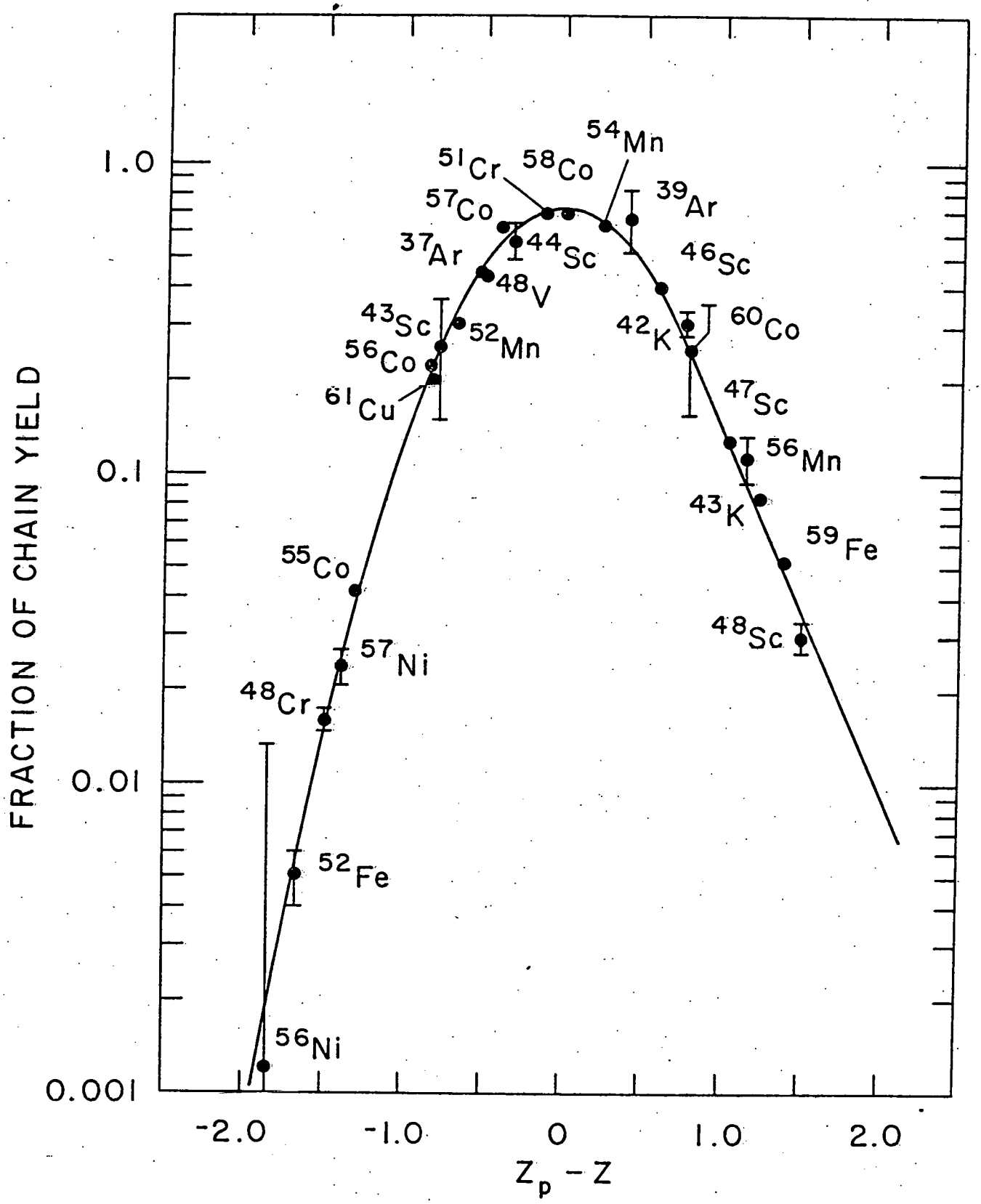
FRACTION OF CHAIN YIELD
1.0
0.1
0.01
0.001
-2.0
-1.0
0
1.0
2.0
$Z_p - Z$
^{54}Mn
^{51}Cr
^{58}Co
^{39}Ar
^{57}Co
^{37}Ar
^{44}Sc
^{46}Sc
^{48}V
^{43}Sc
^{52}Mn
^{42}K
^{60}Co
^{56}Co
^{61}Cu
^{47}Sc
^{56}Mn
^{43}K
^{59}Fe
^{55}Co
^{48}Sc
^{57}Ni
^{48}Cr
^{52}Fe
^{56}Ni

Fig. 3

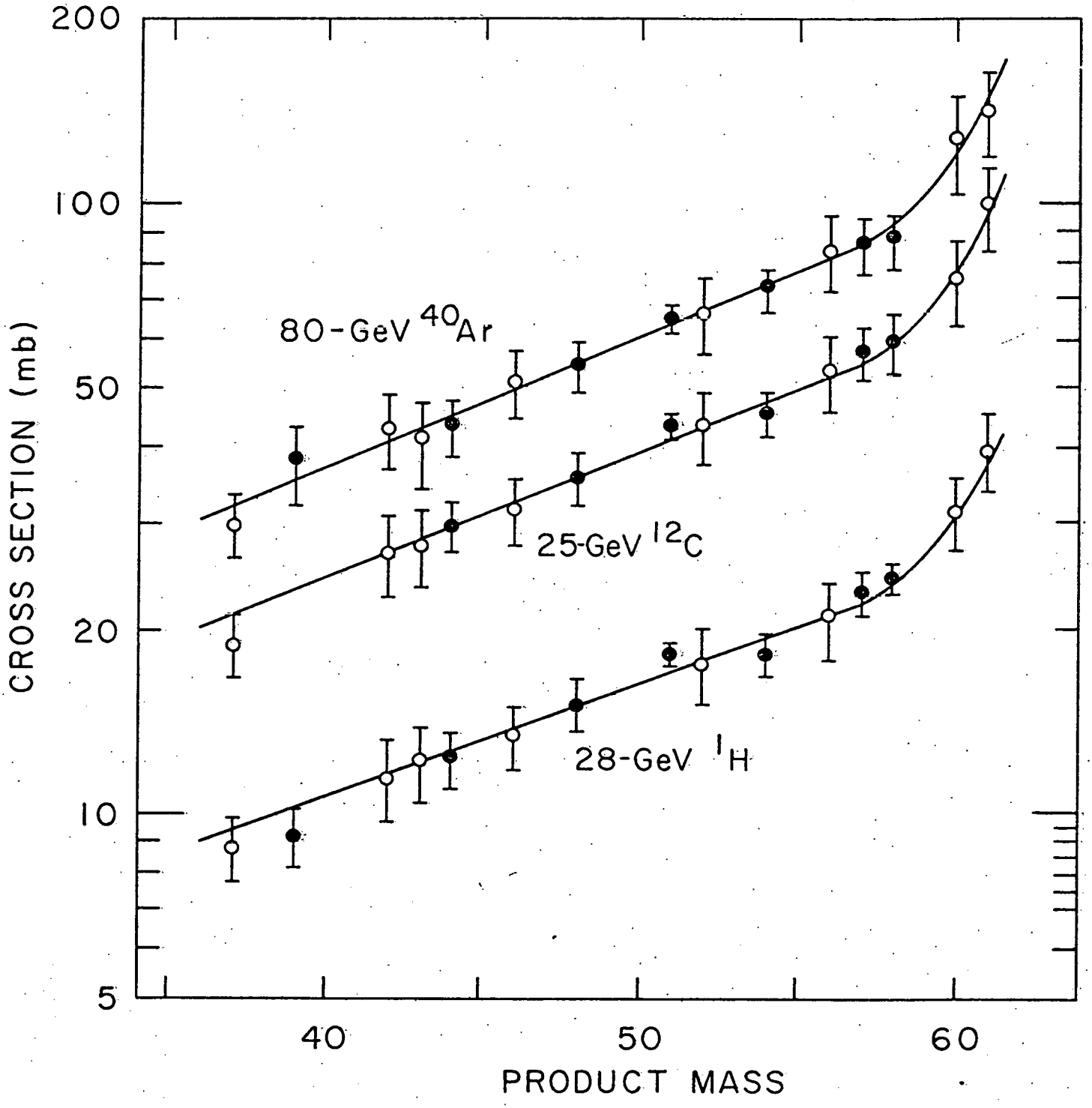
200
100
50
20
10
5
CROSS SECTION (mb)
80-GeV ^{40}Ar
25-GeV ^{12}C
28-GeV ^{1}H
40
50
60
PRODUCT MASS

Fig. 4

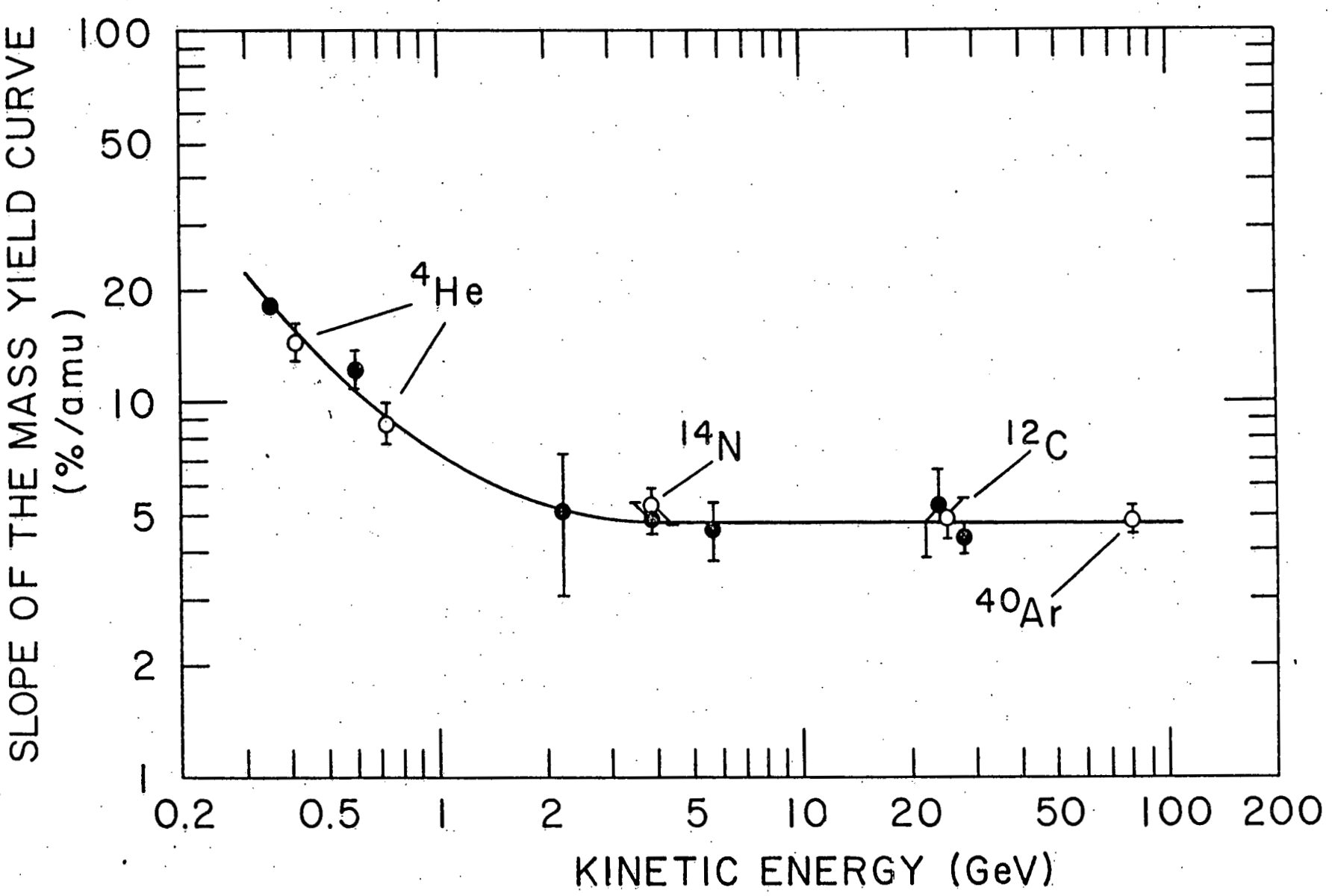

Fig. 5

04-752-79

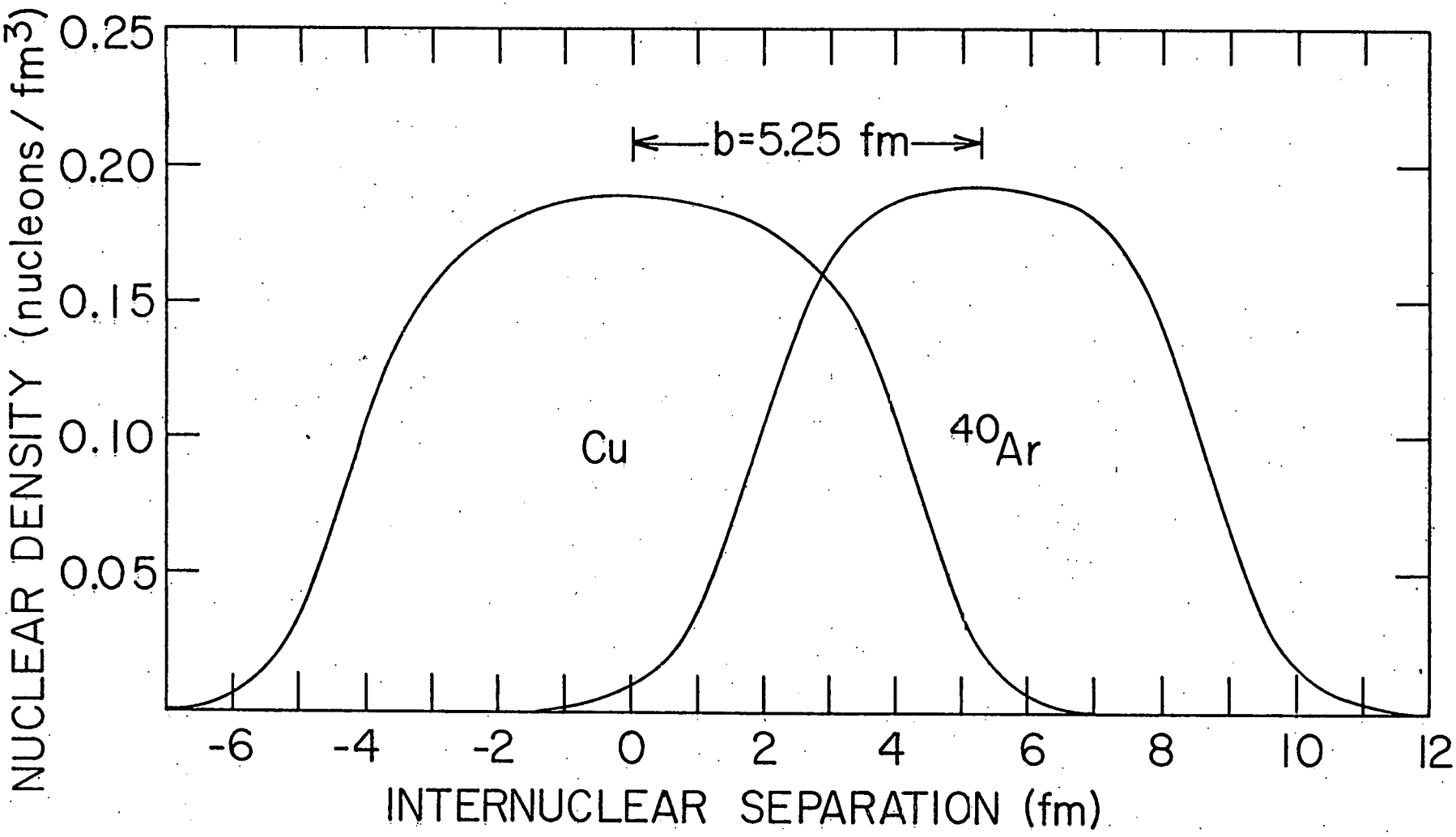

Fig. 6

6-1421-79

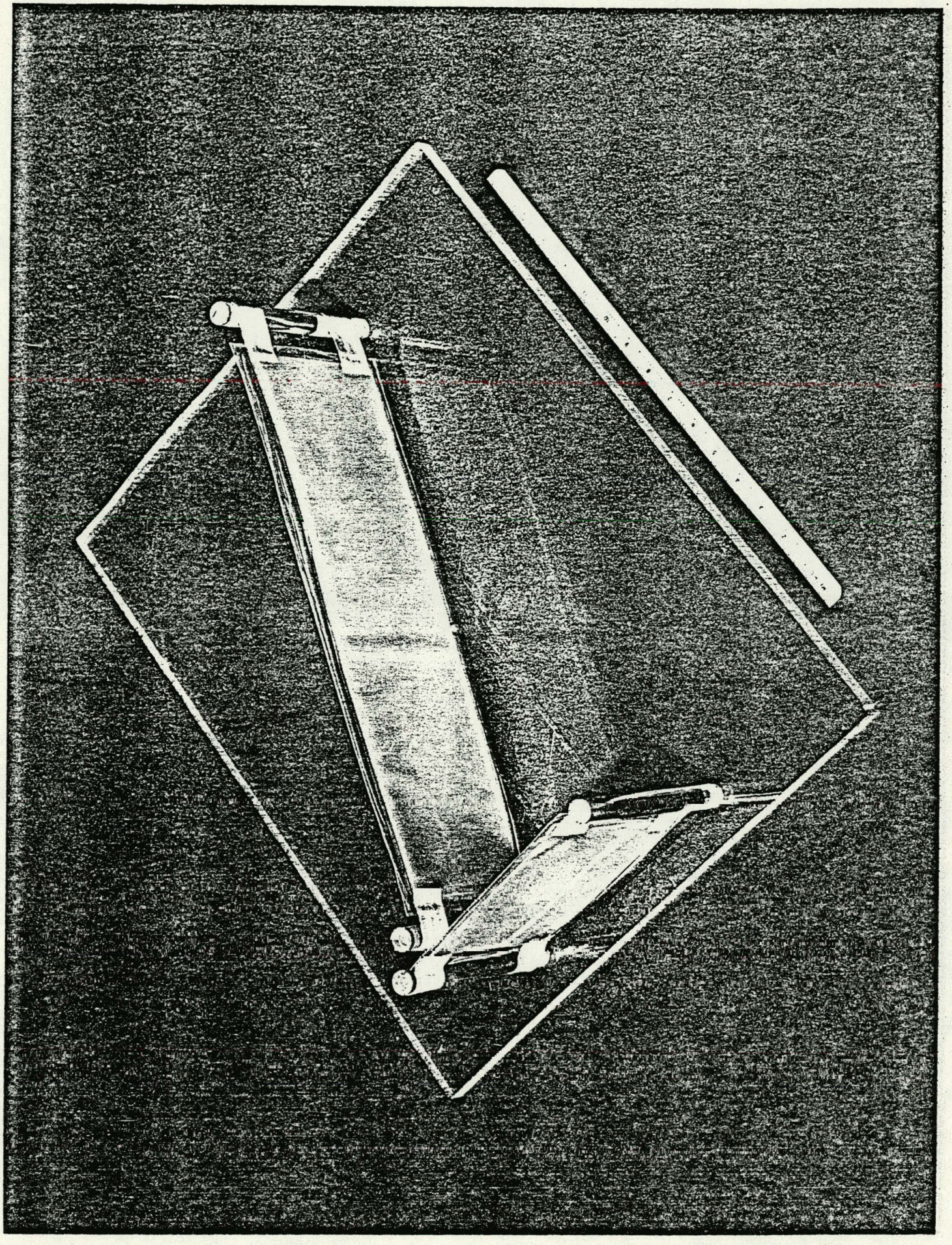

Fig. 7

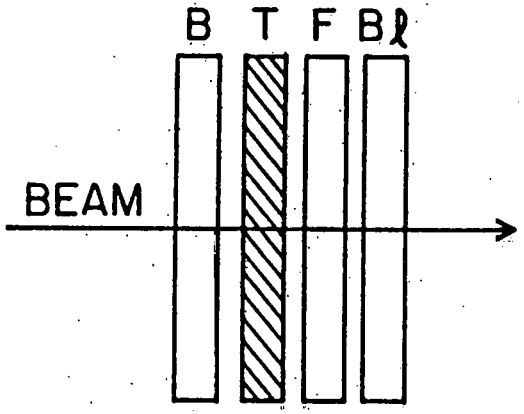

B,F BACKWARD AND FORWARD CATCHERS

T TARGET (w mg/cm^2)

Bℓ BLANK CATCHER

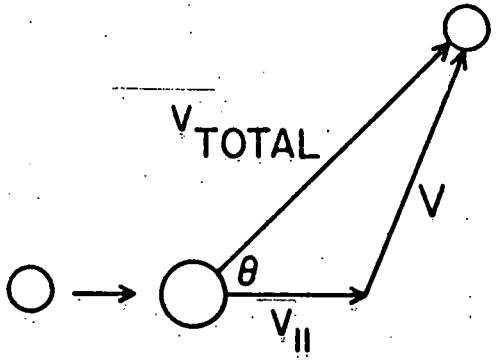

$\langle RANGE \rangle = 2w\,(F+B)$

$\langle \eta_{\parallel} R \rangle = w\,(F-B)$; $\eta_{\parallel} = v_{\parallel}/V$

$R \propto V^N$

Fig. 8

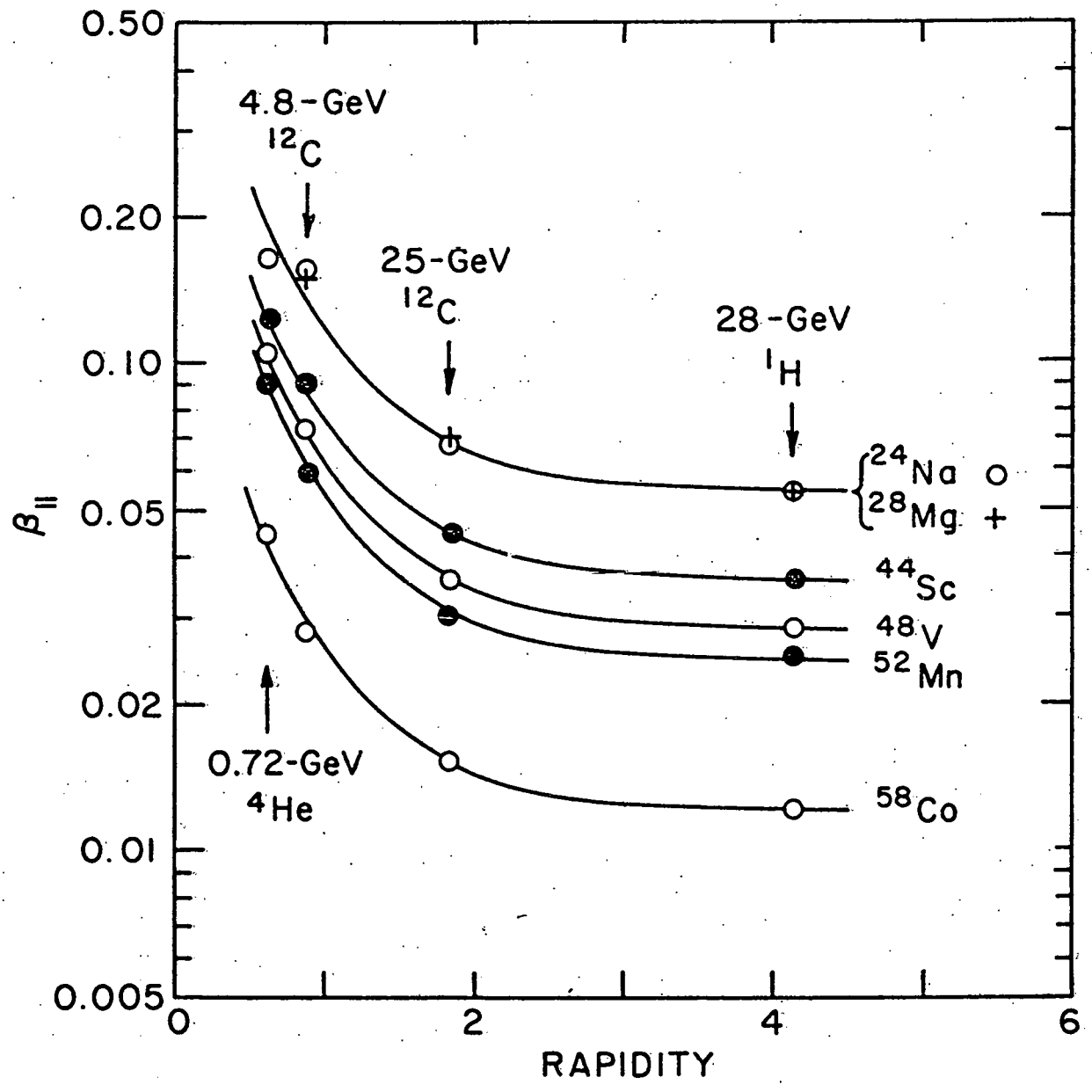
0.50
0.20
0.10
0.05
0.02
0.01
0.005
β_{II}
0
2
4
6
RAPIDITY
4.8-GeV
^{12}C
25-GeV
^{12}C
28-GeV
^{1}H
0.72-GeV
^{4}He
^{24}Na ○
^{28}Mg +
^{44}Sc
^{48}V
^{52}Mn
^{58}Co

Fig. 9

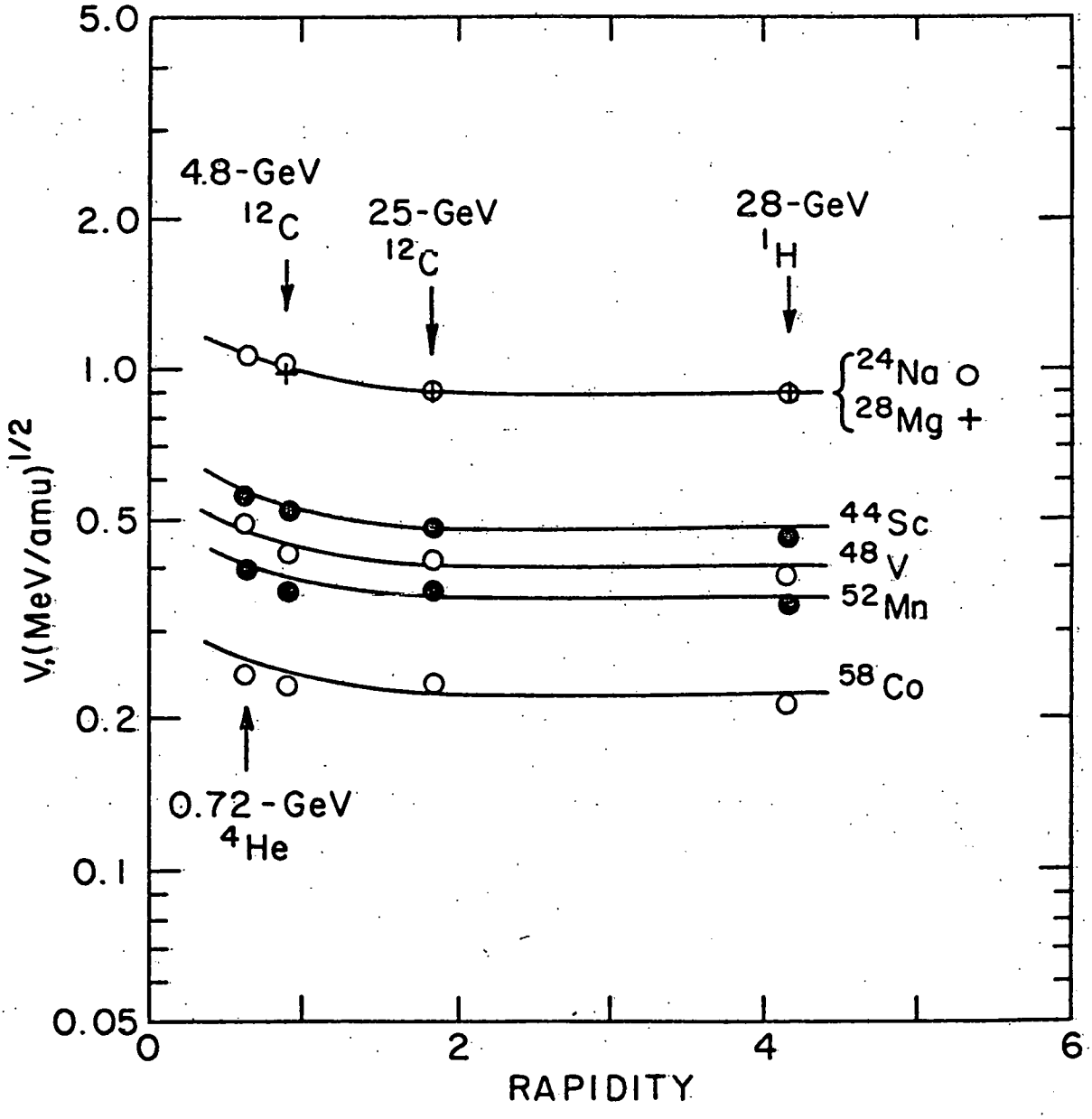
5.0
2.0
1.0
0.5
0.2
0.1
0.05
0
2
4
6
RAPIDITY
V,(MeV/amu)^1/2
4.8-GeV
12C
25-GeV
12C
28-GeV
1H
24Na O
28Mg +
44Sc
48V
52Mn
58Co
0.72-GeV
4He

Fig. 10